ChemComm

Accepted Manuscript

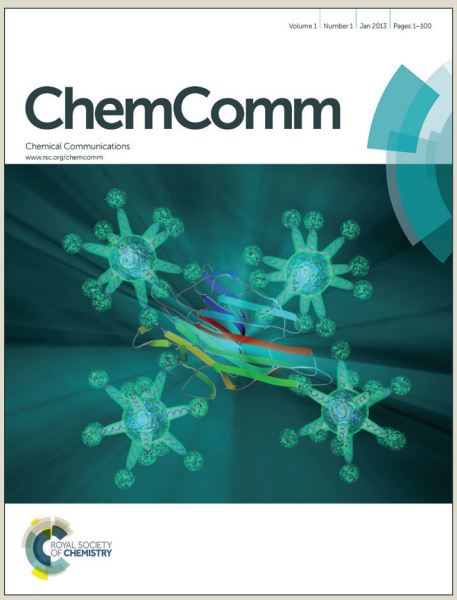

ROYAL SOCIETY OF CHEMISTRY

www.rsc.org/chemcomm

Cite this: DOI: 10.1039/c0xx00000x

www.rsc.org/xxxxxx

COMMUNICATION

Stable amorphous calcium oxalate: Synthesis and potential intermediate in biomineralization

Myriam Hajir[a], Robert Graf[b], and Wolfgang Tremel[a]*

Received (in XXX, XXX) Xth XXXXXXXXX 20XX, Accepted Xth XXXXXXXXX 20XX
DOI: 10.1039/b000000x

Amorphous calcium oxalate nanoparticles with sizes of ≈ 10 nm were synthesized at room temperature by hydrolysis of dimethyl oxalate from ethanolic solution.

A common strategy in biomineralization is the formation of transient amorphous precursor phases that transform subsequently into one of their more stable crystalline counterparts.[1] This process was first observed in the animal kingdom in the radular teeth of molluscs.[2] Amorphous calcium phosphate was identified recently in newly deposited fin bones of zebrafish.[3] Calcium carbonate was observed in different invertebrate phyla.[4-9] Amorphous calcium phosphate and calcium carbonate (ACC) can be synthesized *in vitro* from highly supersaturated solutions.[10-13] The amorphous phases are stable in the dry state, but rapidly transform into the associated crystalline phases in aqueous solution.

The most common types of biominerals in plants are calcium oxalate crystals, calcium carbonate, and silica.[14] In higher plants, calcium oxalate is sequestered within intravacuolar membrane chambers of specialized cells. Calcium is a required element for plant growth and development, and it plays important roles, for example, as a structural component of cell walls[15] or a signal in various physiological and developmental pathways.[16] As the free Ca^{2+} concentration in the cytosol must be kept at a low level to prevent interference with cell processes such as Ca-dependent signaling,[16] phosphate-based energy metabolism,[17] or microskeletal dynamics[18] surplus Ca^{2+} is stored as crystalline calcium oxalate monohydrate (COM, $CaC_2O_4{\cdot}H_2O$, whewellite)[19] or tetragonal calcium oxalate dihydrate (COD, $CaC_2O_4{\cdot}2H_2O$, weddellite).[20,21] Calcium oxalate trihydrate (CaOx, $CaC_2O_4{\cdot}\ 3H_2O$, caoxite)[21] is less prominent. Calcium oxalate in cell walls and the vacuole[22] is a relatively insoluble, metabolically inactive salt for calcium sequestration.[22] Some plants may accumulate calcium oxalate in substantial amounts, up to 80% of their dry weight.[23] Furthermore, calcium oxalates are the main constituents of kidney stones,[24] one of the major health problems worldwide.[25,26]

The mechanistic details of the formation of calcium oxalate, in particular of its phase transformations, are poorly understood. Because of the fundamental role of calcium oxalate, experimental[18-21,27-29] and theoretical[30] studies have been concerned with its crystal structure, formation and growth. A chemical synthesis of the amorphous transient phase may not only help explaining the formation of complex biominerals in living systems, but also shed light on the mechanisms of its crystallization in general. Here, we address this fundamental issue by the synthesis of amorphous calcium oxalate (ACO) through the reaction of $CaCl_2$ x $2H_2O$ with dimethyl oxalate in ethanol in the absence of additives. During the reaction, ACO precipitates on a timescale of 1-3 minutes as determined by UV-vis spectroscopy and light scattering.

In a typical synthesis of ACO 0.1 mmol of calcium chloride dihydrate ($CaCl_2$ x $2H_2O$, 99,99%, Sigma) and 0.1 mmol of dimethyl oxalate $(CH_3)_2C_2O_4$, 99,99% Sigma) were dissolved in 50 mL of absolute ethanol at room temperature. The reaction was initiated by adding 0.2 mmol of NaOH under stirring to the reaction solution. After 2 h a gel-like precipitate (digital images in Fig. 1a,b) had formed which was removed by centrifugation (9000 rpm, 20 minutes) and washed several times with anhydrous ethanol. After vacuum drying for 24 h a thin film (Fig. 1c) containing aggregates of spherical particles with diameters of approx. 10 nm had formed as shown independently by scanning electron microscopy (SEM) and light scattering. For comparison, a reaction using $CaCl_2$ x 6 H_2O and an aqueous dimethyl oxalate solution lead to the formation of a precipitate of COM crystals (Fig. 1a left and Fig. S2, Supporting Information).

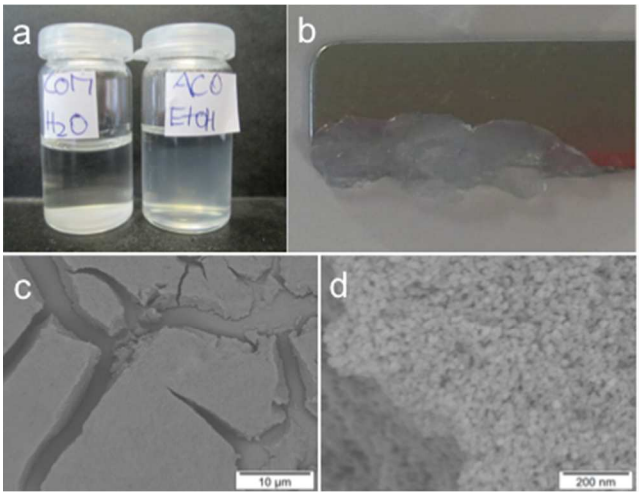

Fig. 1. (q) Precipitation of calcium oxalate by reaction of dimethyl oxalate and $CaCl_2$ x $2H_2O$ in aqueous solution (left) and in anhydrous ethanol (right). (b) A transparent gel-like precipitate was formed in the anhydrous system, whereas crystalline COM was formed in the aqueous system. (c) SEM image of the dried film of amorphous calcium oxalate which contained (d) nanosized (10-30 nm) spherical particles.

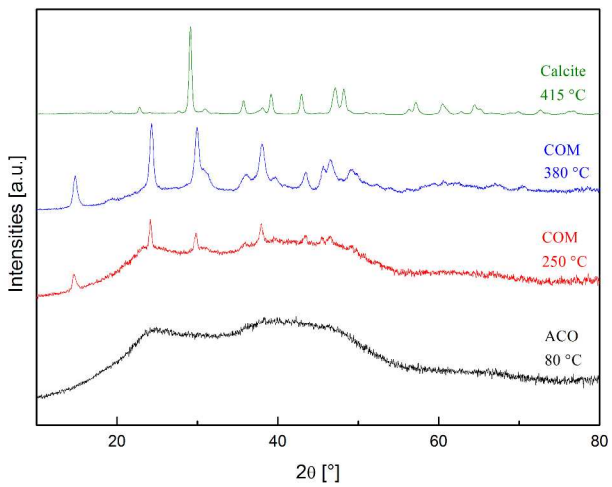

Fig. 2. X-ray diffractograms of ACO (bottom trace) obtained by the reaction of $CaCl_2$ x $2H_2O$ in anhydrous in ethanol and annealing at 80°C and the products obtained after annealing 250°C, 380°C, and 415°C.

The product from the non-aqueous system was amorphous as indicated by the absence of reflections in the X-ray diffractogram (Fig. 2, black trace). The thermal stability of ACO and the phase transition to COM were monitored by X-ray powder diffraction, differential scanning calorimetry (DSC) and thermogravimetry (TG). The thermogravimetric and DSC traces of ACO under nitrogen (Fig. 3) revealed a weight loss of 13.5% in the range from 150-200°C, which was attributed to the loss of water and/or ethanol solvate. The crystallinity of the COM intermediate (PDF 20-0231) increased with temperature (Fig. 2, red and blue trace), the crystallization was complete at ≈ 380°C. Around 400°C an incipient decarbonylation lead to the formation of $CaCO_3$. The formation of calcite was complete at ≈ 415°C, as shown by the exothermic event in the DSC (Fig. 3) and the diffractogram (Fig. 2, green trace). The decarboxylation of $CaCO_3$ at 700°C and the formation portlandite, a mixture of calcium oxide and calcium hydroxide, as final products of the thermal decomposition are apparent from the strong endothermic event between 700 and 800°C and the X-ray powder diffractogram (Fig. S3).

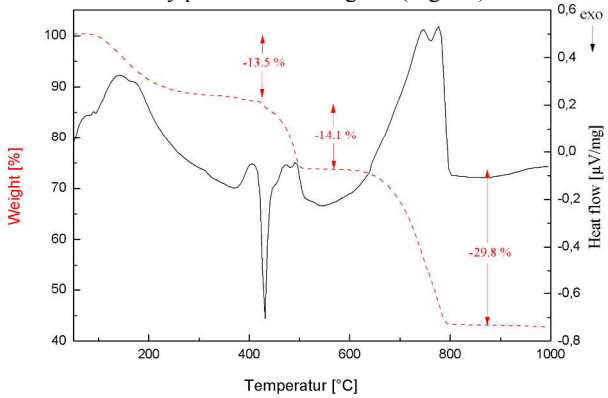

Fig. 3. Thermogravimetric trace (black line) and DTA signal (red line) of ACO under N_2.

Signals observed in both IR (Fig. S4) and Raman spectra (Fig. 4) of ACO can be related to the stretching and bending vibrations of the oxalate groups. The Raman spectra for ACO and a reference sample of COM (Fig. 4, red line and Fig. S5) show bands at 1629 and at 1486, 1465 cm^{-1} for the asymmetric and the symmetric ν(C=O) stretching modes, bands between 850 and 950 cm^{-1} for the ν(C-C) stretching mode band and in the region of 500 cm^{-1} for the deformation $\delta(CO_2)$.[31] The similar band positions of ACO and the reference sample are compatible with a composition CaC_2O_4 x H_2O for ACO. The bands of free oxalate anions and water molecules are split due to factor group splitting and lower site symmetry in the crystal structure of COM (2nd trace, dashed), whereas the spectrum of ACO shows a significant peak broadening, apparent by a higher value for the full width at half maximum (FWHM). These characteristics are representative of highly disordered materials like these amorphous samples. A weak band at 1086 cm^{-1} can be assigned to the C-O stretch of a trace of ethanol, which may act as a solvate molecule in ACO.

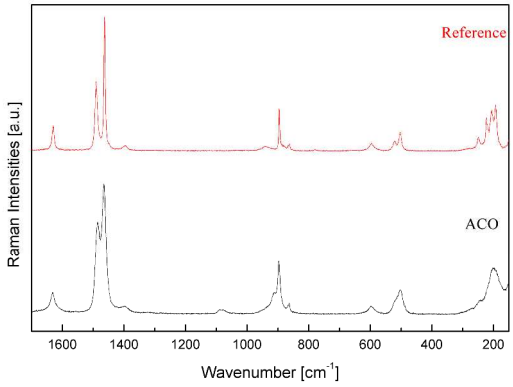

Fig. 4 Raman spectra of COM (reference, top trace) and ACO (bottom trace).

The ^{13}C MAS-NMR spectrum of ACO (black line) shows two broad resonances at 167.9 and 168.7 ppm with a pronounced background between 163 – 172 ppm, whereas for a COM reference sample (red line) four isotropic resonances (FWHM ~ 55 Hz) were observed in agreement with the asymmetric unit of the structure.[18] These four resonances are characterized by similar CSA (see Table 1). Such results are in agreement with those proposed by Bak et al.[32] for calcium oxalate x-hydrate phases ($CaC_2O_4 \cdot xH_2O$). After two months at ambient temperature the sample re-crystallized to calcium oxalate, but only two signals rather than four four could be resolved due to a lack of crystallinity predominates. Ethanol is still present as a trace solvate molecule in ACO as indicated by the IR spectra (Fig. S4)

Our results show that ACO can be synthesized at room temperature from non-aqueous media even without using inorganic or organic additives that would inhibit crystallization by surface complexation.[33,34] ACO could be converted to a mixture of COM and COD in water by ultrasonication. In recent years the early stages of mineral formation, i.e. nucleation and early growth, have received increasing attention as it became evident that not all published data could be reconciled with the classical nucleation and crystallization theory.[35,36] One limitation in quantifying and controlling these early reaction stages is our lack of understanding the processes and variations in the structural identities of the precipitated solids and the mechanisms by which intermediates such as ACO crystallize. The synthesis of the ACO nanoparticles supports the hypothesis that the formation of the metastable amorphous polymorph over the thermodynamically more stable COM (with higher lattice energy) is favored either (i) kinetically

or (ii) because of surface energy.

The precipitation must be carried out in non-aqueous media[37] in order to avoid the precipitation of COM ($K_L = 2.7\times10^{-9}$ mol^{-2}) or the transformation to COM via dissolution-recrystallization. This was demonstrated by carrying out the synthesis in aqueous solution. From a thermodynamic viewpoint the nanoparticles (⌀ ≈ 10 nm) are small enough to allow a crossover in from the crystalline to the amorphous polymorph due to surface energy. The critical size of hydrated ACC for such a crossover has been estimated to ≈ 4 nm.[38]

ACO my serve as a reservoir from which crystalline material can evolve. Furthermore, the crystallization process described here may shed light on the biological crystallization pathway, where COM could be formed (analogous to amorphous $CaCO_3$[39]) in membrane-bound vacuoles, where the binding of transient ACO by the membrane keeps the system free of bulk water.

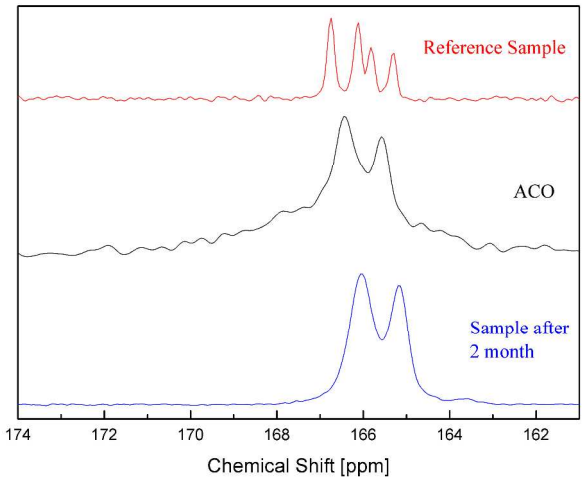

Fig. 4. ^{13}C-MAS-NMR spectra of whedellite (top trace, red), ACO (middle trace, black), both measured at ν_r=25 kHz, and ACO after storing for two month in air (data was measured at ν_r=10 kHz).

Acknowledgements

This study was funded by the Deutsche Forschungsgemeinschaft (DFG) within the priority program 1415. We thank R. Jung-Pothmann for X-ray diffraction measurements and Prof. W. Schärtl for access to the light scattering facilities. The microscopy equipment is operated by the electron microscopy center, Mainz, (EMZM) supported by the Johannes Gutenberg-University and the Max Planck-Institut für Polymerforschung (MPI-P).

Notes and references

[a] Institut für Anorganische Chemie und Analytische Chemie, Johannes Gutenberg-Universität Mainz, Duesbergweg 10-14, D-55099 Mainz.
[b] Max Planck-Institut für Polymerforschung, Ackermannweg 10, 55128 Mainz, Germany

Electronic Supplementary Information (ESI) available: Fig. S1 and S2, SEM and X-ray diffractogram of COM crystals formed in aqueous system. Fig. S3, X-ray diffractogram of thermal decomposition product; Fig. S4 and S5, IR and Raman spectra of ACO.

1 S. Weiner, I. Sagi, and L. Addadi, *Science* 2005, **309**, 1027-1028.
2 K. M. Towe and H. A. Lowenstam, *J. Ultrastruct. Res*. 1967, **17,** 1-13.
3 J. Mahamid, A. Sharir, L. Addadi, and S. Weiner, *Proc. Natl. Acad. Sci. USA* 2008, **105**, 12748-12753.
4 E. Beniash, J. Aizenberg, L. Addadi, and S. Weiner, *Proc. R. Soc. London Ser. B* 1997, **264**, 461-465.
5 B. Hasse, H. Ehrenberg, J. C. Marxen, W. Becker, and M. Epple, *Chem. Eur. J*. 2000, **6**, 3679–3685.
6. J. Aizenberg, G. Lambert, S. Weiner, and L. Addadi, *J. Am. Chem. Soc*. 2002, **124** , 32–39.
7 Y. Politi, T. Arad, E. Klein, S. Weiner, and L. Addadi, *Science* 2004, **306**, 1161–1164.
8 M. J. I. Briones, E. López, J. Méndez, J. B. Rodríguez, and L. Gago-Duport, *Mineral. Mag*. 2008, **72**, 227–231.
9 D. E. Jacob, R. Wirth, A. L. Soldati, U. Wehrmeister, and A. Schreiber, *J. Struct. Biol*. 2011, **173**, 241–249.
10 E. D. Eanes, I. H. Gillessen, and A. S. Posner, *Nature* 1965, **208**, 365–367.
11 F. Betts, N. C. Blumenthal, A. S. Posner, G. L. Becker, and A. L. Lehninger, *Proc. Natl. Acad. Sci. USA* 1975, **72**, 2088–2090.
12 J. Johnston, H. E. Merwin, and E. D. Williamson, *Am. J. Sci*. 1916, **41**, 473.
13 M. Faatz, F. Gröhn, and G. Wegner, *Adv. Mater*. 2004, **16**, 996-1000.
14 H. He, E. J. Ven, J. Kuo, and H. Lambers, *Trends Plant Sci.* 2014, **19**, 166-174.
15 M. Demarty, C. Morvan, and M. Thellier, *Plant Cell Environ*. 1984, **7**, 441–448.
16 D. S. Bush, *Annu. Rev. Plant Physiol. Plant Mol. Biol*. 1995, **46**, 95–122.
17 P. K. Hepler, *Cell Calcium* 1994, **16**, 322-330.
18 M. Daudon, D. Bazin, G. Andre, P. Jungers, A. Cousson, P. Chevallier, E. Veron, and G. Matzen, *J. Appl. Crystallogr*. 2009, **42**, 109-115.
19 A. Frey-Wyssling, *Amer. J. Bot*. 1981, **68**, 130-141.
20 A. Thomas, E. Rosseeva, O. Hochrein, W. Carillo-Cabrera, P. Simon, P. Duchstein, D. Zahn, R. Kniep, *Chem. Eur. J.* 2012, **18**, 4000-4009.
21 T. Echigo, M. Kimata, A. Kyono, M. Shimizu, and T. Hatta. *Mineral. Magazine* 2005, **69**, 77-88.
22 H. Kinzel, *Flora* 1989, **182**, 99-125.
23 E. Zindler-Frank, *Z. Pflanzenphysiol*. 1976, **80**, 1-13.
24 T. Lee and Y. Chen. Lin, *Cryst. Growth Des*. 2011, **11**, 2973-2992.
25 F. L. Coe, A. Evan, and E. Worcester, *Clin. J. Am. Soc. Nephrol*. 2011, **6**, 2083-2092.
26 O. W. Moe, Lancet 2006, **367**, 333-344.
27 S. R. Qiu, A. Wierzbicki, C. A. Orme, A. M. Cody, J. R. Hoyer, G. H. Nancollas, S. Zepeda, and J. J. DeYoreo, *Proc. Natl. Acad. Sci. USA* 2004, **101**, 1811-1815.
28 O. Hochrein, A. Thomas, and R. Kniep, *Z. Anorg. Allg. Chem*. 2008, **634**, 1826-1829.
29 H. Colas, L. Bonhomme-Coury, C. Coelho Diogo, F. Tielens, F. Babonneau, C. Gervais, D. Bazin, D. Laurencin, M. E. Smith, J. V. Hanna, M. Daudon, and C. Bonhomme, *Cryst. Eng. Commun*. 2013, **15**, 8840-8847.
29 D. DiTommasio, S. E. Ruiz Hernandez, Z. Du, and N. H. De Leeuw, *RSC Adv.* 2012, **2** 4664-4674.
30 R. L.Frost, J. Yang, and Z. Ding. *Chin. Sci. Bull*. 2003, **48**, 1844-1852.
31 M. Bak, J. K. Thomsen, H. J. Jakobsen, S. E. Petersen, T-. E. Petersen, and N. C. Nielsen, *J. Urol*. 2000, **164**, 856-863.
32 L. B. Gower, D. J. Odom, *J. Cryst. Growth* 2000, **210**, 719-734.
33 N. Loges, H. A. Therese, K. Graf, L. Nasdala, and W. Tremel, *Langmuir* 2006, **22**, 3073-3080.
34 D. Gebauer, A. Völkel, and H. Cölfen, *Science* 2008, **322**, 1819-1822.
35 D. Gebauer, P. N. Gunawidjaja, J. Y. Peter Ko, Z. Bacsik, B Aziz, L. Liu, Y. Hu, L. Bergström, C.-W.Tai, T.-K. Sham, M. Edén, and N. Hedin, *Ang. Chem. Int. Ed*. 2010, **49**, 8889-8891.
36 T. Schüler and W. Tremel, *Chem. Commun*. 2011, **47**, 5208-5210.
37 A. V. Radha, T. Z. Forbes, C. E. Killian, P. U. P. A. Gilbert, A. Navrotsky, *Proc. Natl Acad. Sci. USA* 2010, **107**, 16438-16442.
38 Y. Politi, R. A. Metzler, M. Abrecht, B. Gilbert, F. H. Wilt, I. Sagi, L. Addadi, S. Weiner, P. U. P. A. Gilbert, *Proc. Natl Acad. Sci. USA* 2008, **105**, 17362-17366.

Stable amorphous calcium oxalate: Synthesis and potential intermediate in biomineralization

*Myriam Hajir, Robert Graf, and Wolfgang Tremel**

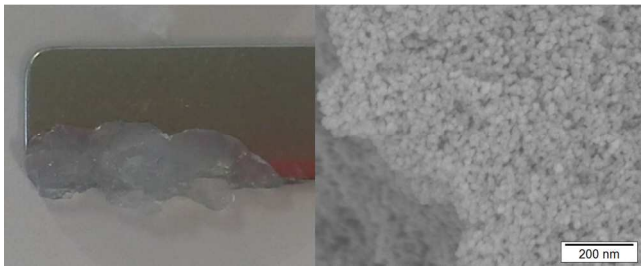

Amorphous calcium oxalate nanoparticles with sizes of 10-30 nm were synthesized at room temperature by the hydrolysis of a dimethyl oxalate from ethanol solution.